

XEROX

Century Data Systems
A Xerox Company

"A SUPERPOSITION BASED ANALYSIS
OF PULSE-SLIMMING TECHNIQUES
FOR DIGITAL RECORDING"

Nigel D Mackintosh, B Sc, Ph D *

Presented at:

IERE Conference on Video and Data Recording
Southampton, England
July 1979

Published in:

The Radio and Electronic Engineer
Vol. 50, No.6
June 1980

* Century Data Systems, P O Box 3056, Anaheim, CA 92803-3056

A superposition-based analysis of pulse-slimming techniques for digital recording

N. D. MACKINTOSH, B.Sc., Ph.D.*

Based on a paper presented at the IERE Conference on Video and Data Recording held at Southampton in July 1979

SUMMARY

The application of pulse-slimming to digital magnetic recording is investigated, and analysed using superposition. Representative criteria are used to determine the maximum achievable packing density both before and after slimming. The results indicate that pulse-slimming is of little value for an already-optimized recording system, but could be used to trade-off timing margin against amplitude margin in a new design.

* Formerly with Racal Recorders Ltd, Hythe, Hampshire, England; now with Burroughs Corporation, Peripheral Products Group, 5411 North Lindero Canyon Road, Westlake Village, California 91361, USA.

1 Introduction

The superposition technique offers an opportunity for many facets of the magnetic recording process to be analysed in non-real time, allowing the recording and replay mechanism to be effectively magnified for greater insight into the detailed changes produced by variation of any of the parameters involved, such as coding technique, packing density, or detection process.

The superposition principle, as applied to magnetic recording, states: 'At all packing densities for which the read-back process is linear, the net flux in the read-coil from any pattern of surface flux-reversals is the algebraic sum of the individual flux contribution from each reversal acting on its own'. This principle provides a very simple means of simulating the effects of any pattern at any packing density, since the isolated reversal response, called here 'the basic pulse', can be stored on a computer as an array of voltage readings, and then any number of these basic pulses can be added or subtracted, at the correct distances from each other, to produce the total output voltage waveform. Measurements can then easily be made on this output waveform to calculate peak-shift, amplitude, etc.

The only phenomena which will render superposition invalid are those which alter the written transition shape in a manner dependent upon the transition density. Morrison and Speliotis¹ report this range of validity to go up to 60 000 bits/in, a packing density out of reach of current technology. Other authors have suggested that this figure is too high, but the alternative to superposition is the dynamic iterative hysteretic model²⁻⁴ which, although more accurate than superposition, particularly at very high packing densities, involves many times the computational effort, and was therefore not considered for this study because of the large number of permutations involved in the analysis.

2 Choice of the Basic Pulse

The heart of the superposition process is the basic pulse, and this must naturally be chosen very carefully. Several expressions have previously been chosen to represent the basic pulse analytically. Hoagland⁵ proposed the Gaussian expression $v(t) = \exp(-t^2)$ which was also used by Chu,⁶ as well as the Lorentzian $v(t) = 1/(1+t^2)$, used also by Kosters and Speliotis.⁷ The mathematical justification for the latter is that the Lorentzian is the derivative of the arctangent function, which has widely been assumed to be a good representation of the magnetization distribution in an isolated transition region.

Sierra^{8,9} has also used the Gaussian expression, whilst Jacoby¹⁰ modified this to $v(t) = \exp(-t^{1.6})$. Several other expressions were also considered by the author.

All the results from the superposition program are normalized to the width of the basic pulse at 50% of the maximum amplitude, i.e. to PW_{50} . The latter is now

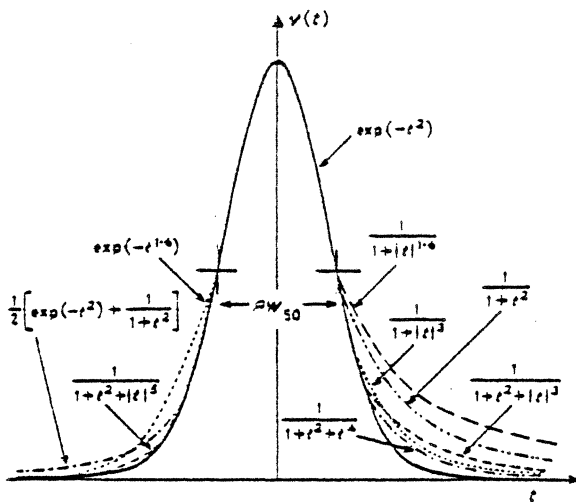


Fig. 1. Analytical basic pulses.

universally accepted as a sound basis of comparison between pulses; it is easily measured in practice due to the high slope of the pulse in this region, and produces much less error when directly comparing pulses than does the more obvious alternative of basewidth, i.e. PW_{50} .

The nine basic pulses used are plotted in Fig. 1. Only one curve is given above the PW_{50} point for clarity, as the curves are all very close in this region. It can be seen that the expressions account for almost any shape of symmetrical pulse likely to be encountered, although even an asymmetrical one can be simulated by using different expressions on each side of the origin.

Several different currently-available memories were used to compare the analytical pulses against, though not simply by comparing practical basic pulse shape against theoretical one, as this cannot be done accurately. Instead, for each of the memories available, graphs were plotted of 'all ones NRZ1 amplitude' and 'two ones NRZ1 peak-shift' against packing density, and similar graphs were produced for each analytical expression using a superposition program. The theoretical graphs were then compared with the practical ones for both location and fit. The clear winner in this comparison was found to be $1/(1+t^2+t^4)$, with $1/(1+t^2+|t|^3)$ and $\exp(-t^2)$ fairly good, but the great surprise was that the Lorentzian came out very poorly.

3 The Pulse-Slimming Principle

Since superposition is normalized to PW_{50} , the implication is that the maximum packing density achievable by any code and/or detection system is inversely proportional to PW_{50} . The possibility of slimming the read-back pulse therefore implies an



Fig. 2. The waveform recovery chain.

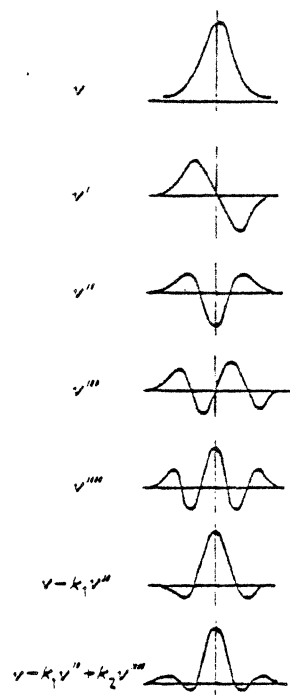


Fig. 3. Pulse-slimming by addition of derivatives.

increase in the packing density and storage capacity of a given store. This must certainly be true if the slimming is effected 'mechanically', e.g. by reducing the head-to-surface separation or oxide coating thickness, but the validity of the theory of superposition also allows the slimming to be performed electronically, after the data waveform has been read back from the surface. The pulse-slimming filter then merely represents an extra block in the recovery chain, as shown in Fig. 2.

4 Addition of Derivatives

Figure 3 shows how a symmetrical pulse (v) suffers a reduction in PW_{50} by the subtraction of its second derivative (v''), in the correct proportion, but also contains significant baseline undershoot. The further addition of a proportion of the fourth derivative (v'''') to this reduces the undershoot, but also introduces overshoot as shown. If the initial pulse is substantially asymmetrical, odd-order derivatives may be applied to correct this, though this extra complication will not be considered here.

Figure 4 shows the effect of the addition of $-v''$ to v in various proportions, using the superposition program. The two pulses are first normalized so that the peak amplitude of each is unity. They are then added, and the resulting slimmed pulse is also normalized. Its PW_{50} and undershoot amplitude are then measured.

4.1 Differentiation

Of particular importance to this pulse-slimming technique is the differential process. The most accurate way of producing the derivatives of the read-back

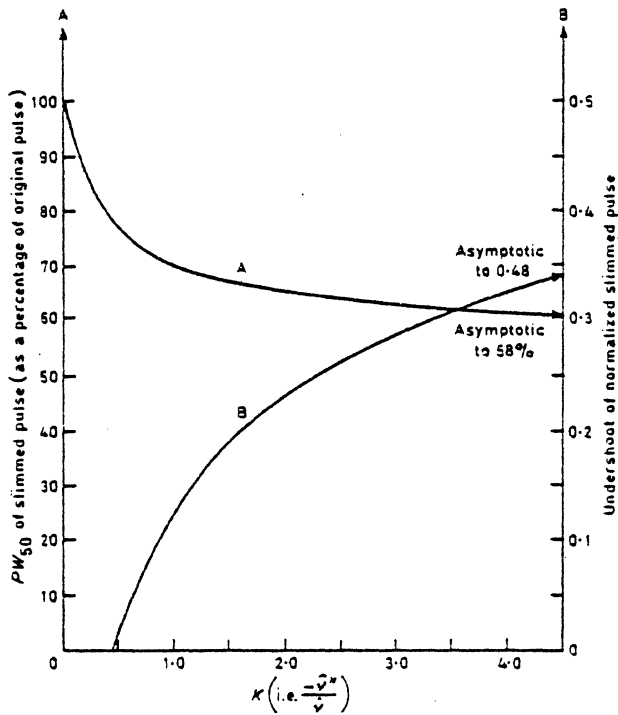


Fig. 4. PW₅₀ and undershoot of slimmed pulse.

waveform involves the use of a delay line. This process can be analysed as follows:

Consider a small portion of the read-back waveform (Fig. 5).

If $v = f(t)$, then

$$v + \delta v = f(t + \delta t)$$

so

$$\begin{aligned} \delta v &= f(t + \delta t) - v \\ &= f(t + \delta t) - f(t). \end{aligned}$$

Therefore

$$\delta v / \delta t = [f(t + \delta t) - f(t)] / \delta t$$

or

$$dv/dt = \lim_{\delta t \rightarrow 0} \{ [f(t + \delta t) - f(t)] / \delta t \}.$$

This shows that the derivative of the read-back waveform can be formed by subtracting from it a delayed version of itself, and the shorter the delay is, the more accurate will be the differentiation. Unfortunately, any noise superimposed on the signal which is of a higher frequency than the signal fundamental, but not high enough that it can be filtered off, will be doubled in the

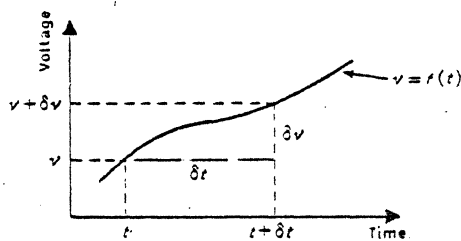


Fig. 5. Read-back waveform.

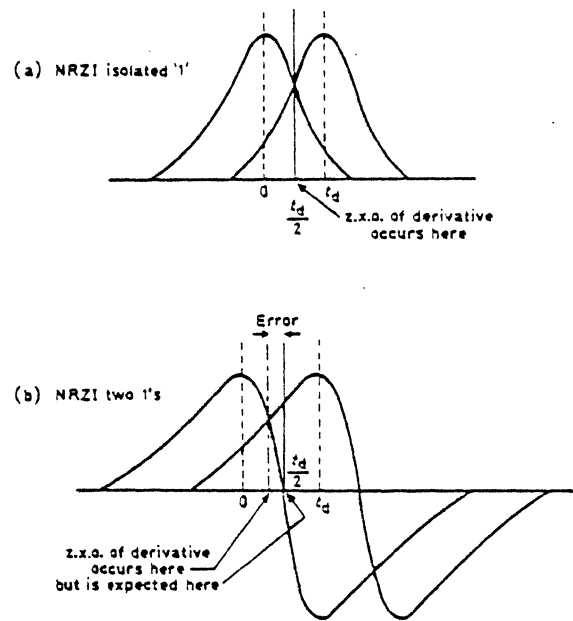


Fig. 6. Worst-case timing error due to non-ideal differentiation.

worst case, as its period will be much less than the delay, and one noise peak could reinforce another. Since the amplitude of the signal derivative falls as the delay is reduced, a compromise must be found between accuracy of differentiation and signal-to-noise ratio.

Figure 6 shows how the accuracy problem arises in practice. For an isolated basic pulse as in (a), the zero-crossing (z.x.o.) of the derivative always occurs at t_d/2 for all values of t_d (the delay between the two signals), assuming the pulse is symmetrical. For the worst case pattern of two ones NRZI (two isolated transitions), shown in (b), however, the steep gradient on one side of the peak and the gentle gradient on the other combine to give a z.x.o. which is not at t_d/2. It is apparent that reducing t_d reduces the error. It should also be noted that, for a given t_d, increasing the packing density will increase the error, as the two gradients mentioned will differ by even more.

The superposition program can again be used to give quantitative answers to this effect. The results of this analysis are shown in Fig. 7, which plots the maximum timing error (as a function of PW₅₀) and the peak amplitude of the derivative of the normalized basic pulse for all values of delay up to 1.0 × PW₅₀.

It is suggested that a suitable trade-off between accuracy and S/N ratio results from using a delay of 0.3 × PW₅₀. This yields a maximum timing error of 0.5% PW₅₀ at PF = 1.5, and a peak signal of 0.4 after differentiating an isolated normalized basic pulse. Since the noise has doubled, note that the S/N ratio has been reduced by 14 dB, though the actual extent to which this loss is felt depends on the particular implementation involved. It is clear, however, that the second derivative will have a very poor S/N ratio, and clearly use of the fourth derivative, whilst beneficial in theory, will not be

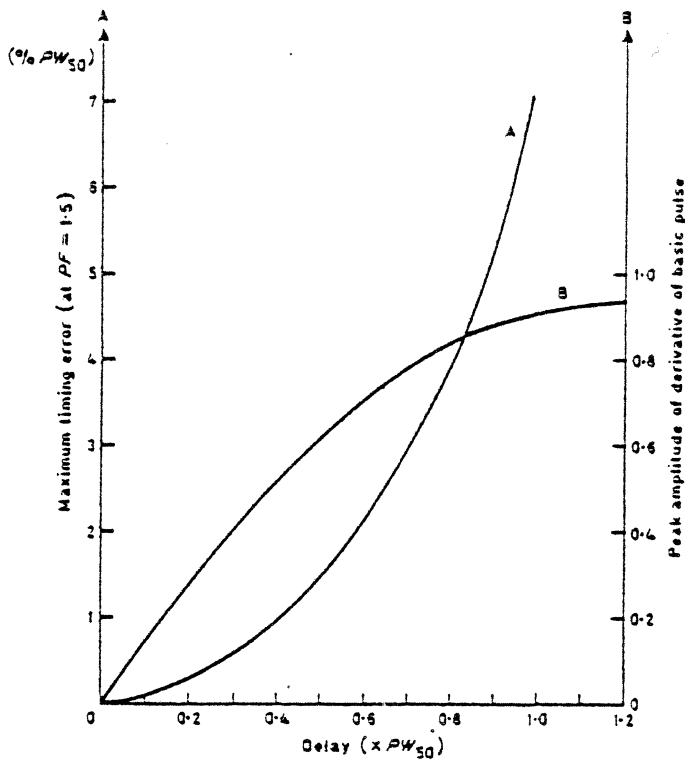


Fig. 7. The effect of using different length delay lines for differentiation.

sensible in practice.

It should be noted that the value of delay suggested above should be selected with reference to the worst-case PW_{50} in a particular system. This means that for pulses with smaller PW_{50} , the effective delay to them is greater than optimum, resulting in a greater timing error, but because these pulses are non-worst-case to start with, they should be able to accommodate this extra error.

4.2 Implementation

The circuit shown in Fig. 8 shows an experimental implementation of this pulse-slimming technique. The short-circuited lumped delay lines perform the differentiation. The delay in the path of the input pulse is to align it correctly with the doubly-differentiated one, which is delayed by $2 \times t_d$ (where t_d is the length of the delay line) relative to its input. The delays are variable (in finite

steps) to enable them to be set correctly relative to the PW_{50} of the input pulse. The variable-gain amplifier, the inverter and the summer can all be effected by means of a high-bandwidth dual-beam oscilloscope with trace-addition facilities.

4.3 Effect on Achievable Packing Density

It was shown in Fig. 4 that the maximum possible reduction in PW_{50} using only the second derivative is 42%, so it would not seem likely that packing density increases will exceed this figure. Indeed, if the slimmed pulse was exactly the same shape as the original pulse, and the S/N ratio was unaltered, the calculation would be as simple as that, but the very complex nature of the slimmed pulse means that only detailed practical or theoretical analysis can determine the exact effect on the achievable packing density.

The first step in this process is to find a packing density limit for a given system before slimming is applied. In this instance, this was done using the superposition program, by calculating worst-case peak-shift and amplitude data for a hypothetical recording system using NRZ1, with a read-back S/N ratio of 20:1 (26 dB), i.e. isolated basic pulses have a peak amplitude of unity, whilst the noise has a peak amplitude of 0.05. The detection system postulated was a typical rectify-and-clip process, as shown in Fig. 9. The read-back waveform is first amplified—this may be automatic gain-controlled amplification, but, if so, perfect a.g.c. action will be assumed. The signal is next full-wave rectified, and then clipped to remove baseline noise, which would otherwise be a problem later on, in the squaring process. A certain amount of the noise could be filtered out by correct choice of the frequency response of the linear amplifier, but a problem arises when the noise has components at frequencies lower than the maximum significant frequency in the data. Attempted filtration of these components will result in integration of the data waveform, having the effect of increasing the PW_{50} of the basic pulses, which clearly limits performance.

Waveforms pertinent to this detection system are shown in Fig. 10 for the worst-case amplitude pattern of

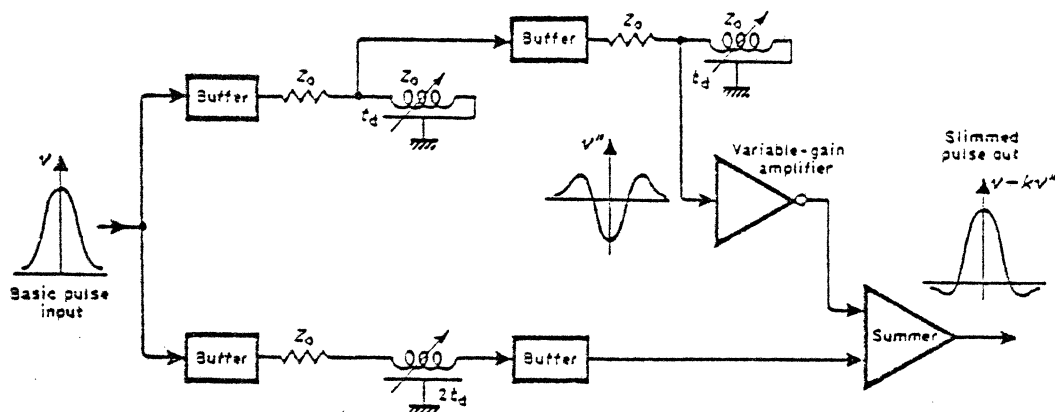


Fig. 8. Active pulse-slimming filter (by addition of derivatives).

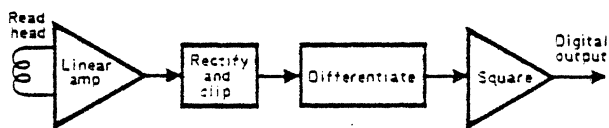
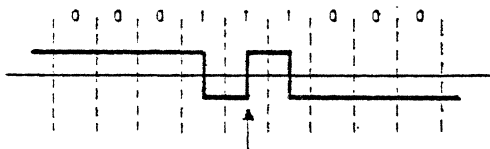


Fig. 9. Rectify-and-clip detection system.

three isolated ones. For the determination of the absolute limit of the system, no margins are allowed, and so the clip level is set to the noise level of 0.05. The differentiation circuit uses a delay line of total delay $0.3 \times PW_{50}$, as described earlier. The signal is finally squared to exaggerate the zero crossovers, which are then detected using the ideal timing window of half a bit period.

The packing density achievable using this detection system may be limited by timing problems or amplitude problems. An amplitude limit will occur where the worst-case read-back signal falls to the clip level of 0.05. Figure 11 is a plot, computed by superposition, of the minimum read-back signal against packing factor (PF), where PF is the packing density normalized to a bit period (BP) equal to PW_{50} , i.e. $PF = PW_{50}/BP$. The peak producing this worst-case signal is the centre '1' of three isolated 1's, i.e.



It can be seen from the graph that zero amplitude margin occurs at $PF = 1.88$.

A timing limit will occur where the worst-case peak shift plus the differentiator error equals half the timing window. Figure 12 shows the worst-case NRZ1 peak-

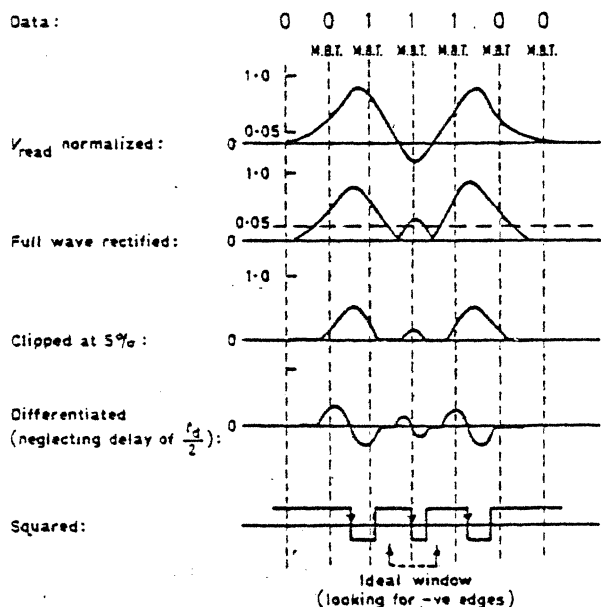


Fig. 10. Rectify-and-clip detection waveforms.

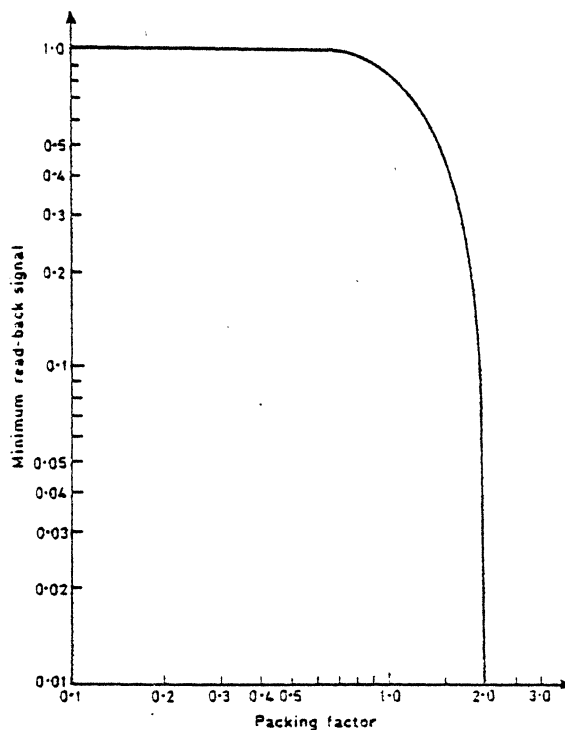


Fig. 11. Minimum read-back signal vs. packing factor for NRZ1 'three-ones'.

shift (for a two 1's pattern) against PF, as calculated by superposition. Zero timing margin occurs where peak-shift = 50% BP, i.e. at $PF = 2.33$. Clearly, the theoretical limit for this code with this detection system occurs at $PF = 1.88$ (due to the three 1's pattern).

No allowance has been made so far for clocking inaccuracies due to such factors as crosstalk, differentiator error, incomplete erasure, particle noise and phase-lock-loop errors, all of which can occur in a practical system. Additionally a practical system would always work with a certain margin on top of the known inaccuracies. Taking a figure of 8% PW_{50} as a reasonable allowance for inaccuracies plus margin, it is possible to calculate a new timing limit for the system. A curve

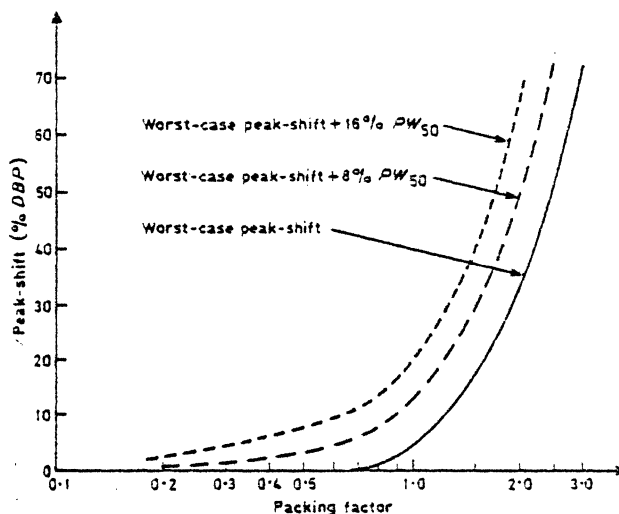


Fig. 12. Worst-case peak-shift for NRZ1.

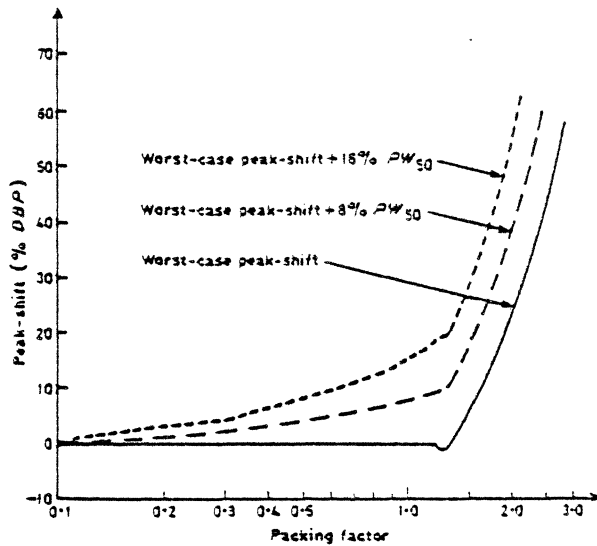


Fig. 13. Worst-case NRZI peak-shift for the slimmed pulse ($v-v'$).

representing this real-time error (RTE) on top of the worst-case peak-shift is shown in Fig. 12, from which it can be seen that the new timing limit is at $PF = 1.92$. A similar construction can be performed for any value of RTE, and if 16% PW_{50} were allowed, for example, the timing limit would be at 1.62.

To summarize these results for clarity:

- (a) $RTE = 0$: Although the timing limit is 2.33, an amplitude limit occurs first at 1.88.
- (b) $RTE = 8\% PW_{50}$: Again, although timing does not limit performance until 1.92, an amplitude limit occurs at 1.88.
- (c) $RTE = 16\% PW_{50}$: Timing causes breakdown first in this case at 1.62.

Consider now a slimmed pulse based on the ratio $v:v' = 1:k$. Assuming, as before, a read-back noise amplitude of 0.05, then allowing again for a doubling of the noise in each differentiator, it can easily be calculated that the peak noise amplitude out of the slimmer is $[0.05 + 0.47k]/(1+k)$, after normalization of the slimmed

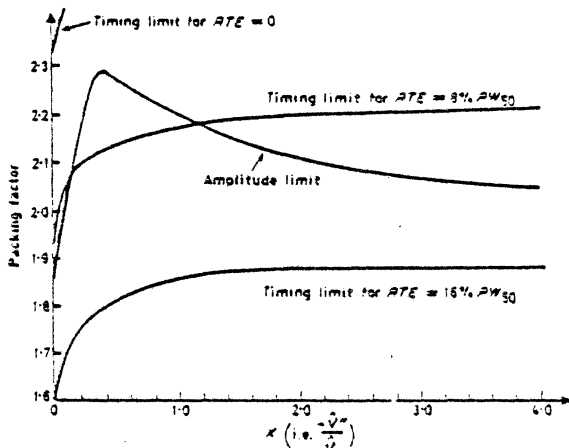


Fig. 14. Timing and amplitude limits after pulse slimming.

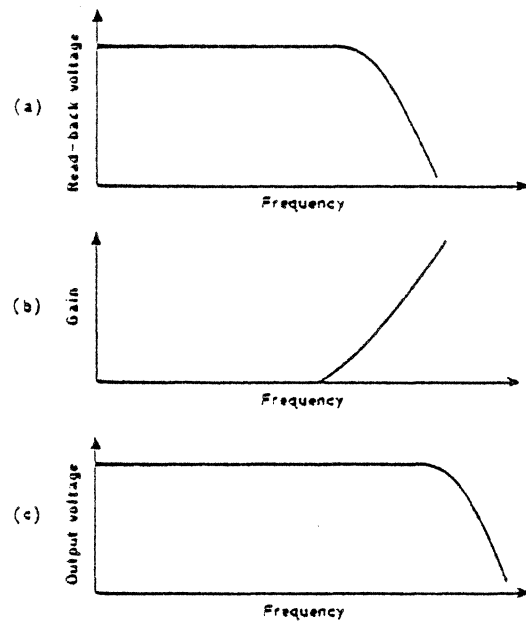


Fig. 15. Pulse-slimming by amplitude compensation. (a) Replay response; (b) Filter characteristic; (c) Improved replay response.

pulse. For $k = 1$, the noise amplitude is 0.26 (compared with undershoot at this stage of 0.12).

The clip-level in the detection system must be set to (at least) the undershoot amplitude plus the noise amplitude to avoid erroneous triggering, i.e. clip-level to be $0.26 + 0.12 = 0.38$. An amplitude breakdown occurs at $PF = 2.20$, where the amplitude of the all-ones pattern (not the usual three 1's pattern), after slimming, falls to 0.38. The worst-case peak-shift pattern changes also. It becomes the three 1's pattern, whose outer peaks' peak-shift is plotted in Fig. 13.

The new packing density limits can be summarized as follows:

- (a) $RTE = 0$: Although the timing limit is at 2.57, an amplitude limit occurs at 2.20 (cf. 1.88 before slimming).
- (b) $RTE = 8\% PW_{50}$: The timing limit now precedes the amplitude limit, and is at 2.15 (cf. 1.88).
- (c) $RTE = 16\% PW_{50}$: Again the timing limit causes breakdown, at 1.86 (cf. 1.62).

The same analysis can now be applied to other slimmed pulses to determine an optimum value of k . Figure 14 shows the results of this analysis, and it can be seen how k can often be chosen to produce simultaneous amplitude and timing breakdowns, thus maximizing the system margins. Summarizing:

- (a) $RTE = 0$: Although the timing limit is never less than 2.32, an optimum amplitude limit occurs for $k = 0.4$, at $PF = 2.29$.
- (b) $RTE = 8\% PW_{50}$: The optimum value of k is 1.2, yielding simultaneous amplitude and timing margins at 2.18.

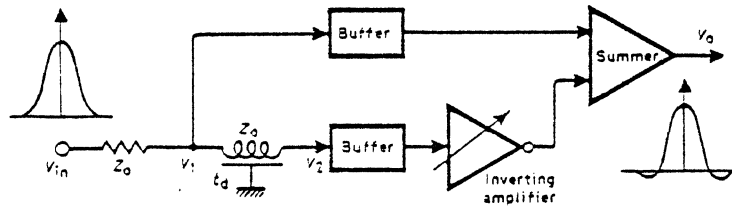


Fig. 16. Active pulse-slimming filter (by amplitude compensation).

(c) $RTE = 16\%$ PW_{50} : The amplitude limit is greater than the timing limit for all values of k , and the timing limit = 1.88 for $k > 1.6$, so the best choice is $k \approx 1.6$, yielding maximum amplitude margin.

The striking shape of the curves in Fig. 14 for $k < 0.4$ deserves some explanation. All the curves show a significant improvement in this area, which then rapidly reduces, or even reverses. Reference to Fig. 4 again shows why this happens: the largest improvement in PW_{50} occurs for $k < 0.4$, after which point not only does the slimming improvement reduce, but also undershoot commences, and increases fairly rapidly. It is apparent then that $k = 0.4$ will generally prove to be optimum, over a wide range of RTE values, resulting in typical packing density increases of 15%.

5 Amplitude Compensation

The basis of this method is the all-ones response shown in Fig. 15(a). If the read-back signal is passed through a filter having the complementary response shown in (b), the result will approach the characteristic shown in (c), giving a greater bandwidth. Since the 3 dB point is being increased, the implication is that inter-symbol interference is being reduced and thus peak shift will be reduced.

One of the best ways of achieving the required gain characteristic is by the use of transversal filters. This is the name given to a class of transmission line devices which afford constant delay, or linear phase, filtering. In practice, a simple lumped delay line provides this effect. A typical implementation of this technique is shown in Fig. 16. The circuit can be easily analysed:

$$V_1 = V_{in} \times Z_s / (Z_s + Z_0)$$

where Z_s is the sending-end impedance of the delay line, and Z_0 is its characteristic impedance

$$V_2 = V_1 / \cos \theta$$

where $\theta = \omega t_d$, and t_d is the electrical length of the line. Therefore

$$\begin{aligned} V_0 &= V_1 - kV_2 \\ &= V_1 - kV_1 / \cos \theta \\ &= V_1(1 - k \sec \theta) \\ &= V_{in}(1 - k \sec \theta) \times Z_s / (Z_s + Z_0) \end{aligned}$$

Since

$$Z_s = -j Z_0 \cot \theta$$

then

$$\begin{aligned} V_0 / V_{in} &= -j \cot \theta (1 - k \sec \theta) / (1 - j \cot \theta) \\ &= (k - \cos \theta)(j \sin \theta - \cos \theta). \end{aligned}$$

Therefore

$$|V_0 / V_{in}| = k - \cos \theta.$$

This has the cosinusoidal form shown in Fig. 17, from which it is apparent that for $\omega t_d < \pi$, i.e. $\omega < \pi / t_d$, the required frequency response is obtained.

However, the circuit can also be analysed in a different manner. With reference to Fig. 15 again:

$$V_1(t = 2t_d) = V_1(2t_d) = 0.5V_{in}(2t_d) + 0.5V_{in}(0)$$

and

$$V_2(2t_d) = V_{in}(t_d)$$

so

$$\begin{aligned} V_0(2t_d) &= V_1 - kV_2 \\ &= 0.5V_{in}(2t_d) + 0.5V_{in}(0) - kV_{in}(t_d). \end{aligned}$$

Letting $k = 1 + c/2$,

$$\begin{aligned} 2 \times V_0(2t_d) &= V_{in}(2t_d) + V_{in}(0) - 2V_{in}(t_d) - cV_{in}(t_d) \\ &= (V_{in}(2t_d) - 2V_{in}(t_d) + V_{in}(0)) - cV_{in}(t_d) \end{aligned}$$

Therefore,

$$2V_0 = V_{in}''(0) - cV_{in}(t_d).$$

This method is therefore shown to be exactly the same as the previous pulse-slimming technique, involving the addition of v and v'' in the appropriate ratio (remember that v is delayed by t_d to align it correctly with v'').

6 Lattice Filters

This is, notionally, a different method, involving postulating the effect of a filter on the isolated pulse, deducing the transfer function of the network, and then, by Laplace transform techniques, realizing the filter with inductors, capacitors and resistors. In effect, however, the method can be viewed as another attempt at amplitude compensation without recourse to transversal filters.

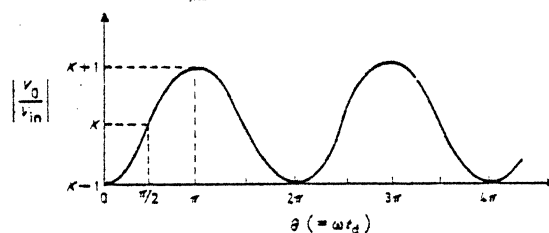


Fig. 17. Pulse-slimming filter characteristic.

Sierra⁹ has described a passive, symmetrical lattice filter for slimming the width of a Gaussian pulse by a factor of two. Although the design aim was a 50% reduction in PW_0 , and presumably PW_{50} , the results show a much less reduction achieved, which would seem to indicate that the limits of this method are akin to those of the two methods already described. Also, since the lattice contains 24 accurate passive components, including inductors, and is a delicately balanced bridge structure, it would seem a less attractive technique than the others.

A simple active equivalent to the symmetrical lattice was investigated by Dodd¹¹ and by Whitehouse.¹² The active circuit reduces the number of complex filter-arm impedances by a factor of four, which clearly benefits a parallel system. None of the three authors mentions the effect of the filter on noise or undershoot, but it would appear from the photographs supplied that this method is hampered by these effects to the same extent as in the addition of derivatives technique. Also, the three authors appear intent on reducing the pulse-width as much as possible. As has been shown, a PW_{50} reduction of 42% is possible (and maybe more using, say, the fourth derivative), but this is not necessarily the optimum choice.

7 Slimming of Asymmetrical Pulses

Many magnetic recording devices, particularly 'in-contact' ones, produce markedly asymmetrical pulses, due primarily to the shape of the transition region in the media, and the influence of the vertical component of magnetization from the media.

A similar analysis to the foregoing shows that the improvements to be obtained on asymmetrical pulses are not as great as those which can be achieved with symmetrical ones. In general, the more asymmetrical the pulse, the less the improvement achievable by slimming. This can be explained with reference to Fig. 18. With a symmetrical pulse, the undershoots on each side of the slimmed pulse are of equal amplitude, and since it is the maximum value of the undershoot which contributes to

breakdown, this is optimum. With an asymmetrical pulse of equal PW_{50} , then, after slimming, one undershoot is smaller, and one larger, than those for the symmetrical pulse. This causes earlier breakdown. One other way of viewing this is that an asymmetrical pulse is already an asymmetrically slimmed version of a symmetrical pulse, thus leaving less margin for extra slimming.

8 Conclusions

It has been shown how superposition can be effectively used to analyse many facets of the magnetic recording process. An analysis of pulse-slimming techniques has shown that only small increases in packing density are possible by their use. Improvements up to 20% are obtainable, though it is doubtful whether such a small improvement is worthwhile for a system already in operation. It may be beneficial, however, to use pulse-slimming to trade off amplitude margin against timing margin, or vice-versa, particularly in the design of a new system, where it may also be possible to radically alter the detection process to cater for the peculiar type of waveform distortion produced by the pulse-slimming.

9 Acknowledgments

The author wishes to thank the Science Research Council and the University of Manchester for sponsoring this study.

10 References

- 1 Morrison, J. R. and Speliotis, D. E., 'Study of peak-shift in thin recording surfaces', *IEEE Trans. on Magnetics*, MAG-3, no. 3, pp. 208-11, September 1967.
- 2 Chi, C. S. and Speliotis, D. E., 'Dynamic self-consistent iterative simulation of high bit density digital magnetic recording', Intermag 1974, *IEEE Trans. on Magnetics*, MAG-10, no. 3, pp. 765-68, September 1974.
- 3 Speliotis, D. E., 'Digital recording theory', *Annals N.Y. Acad. Sci.*, 189, pp. 21-51, January 1972.
- 4 Curland, N. and Speliotis, D. E., 'An iterative hysteretic model for digital magnetic recording', *IEEE Trans. on Magnetics*, MAG-7, no. 3, pp. 538-43, September 1971.
- 5 Hoagland, A. S., 'Digital Magnetic Recording' (Wiley, New York, 1963).
- 6 Chu, W. W., 'Computer simulation of waveform distortions in digital magnetic recordings', *IEEE Trans on Electronic Computers*, EC-15, no. 3, pp. 328-36, June 1966.
- 7 Kusters, A. J. and Speliotis, D. E., 'Predicting magnetic recording performance by using single pulse superposition', Intermag 1971, *IEEE Trans. on Magnetics*, MAG-7, no. 3, pp. 544, September 1971.
- 8 Sierra, H. M., 'Bit shift and crowding in digital magnetic recording', *Electro-technology (U.S.A.)*, 74, no. 9, September 1966.
- 9 Sierra, H. M., 'Increased magnetic recording readback resolution by means of a linear passive network', *IBM J. Res. Develop.*, 7, no. 1, pp. 22-33, January 1963.
- 10 Jacoby, G. V., 'High Density Digital Magnetic Recording Techniques', RCA EM-6224, March 1964.
- 11 Dodd, P. D., 'A simple active equivalent to a lattice pulse-slimming filter', *IBM J. Res. Develop.*, 7, no. 3, pp. 257-8, July 1963.
- 12 Whitehouse, A. E., Ph.D. thesis, University of Manchester, 1970.

Manuscript received by the Institution in March 1979.
(Paper No. 1940/CC 330)

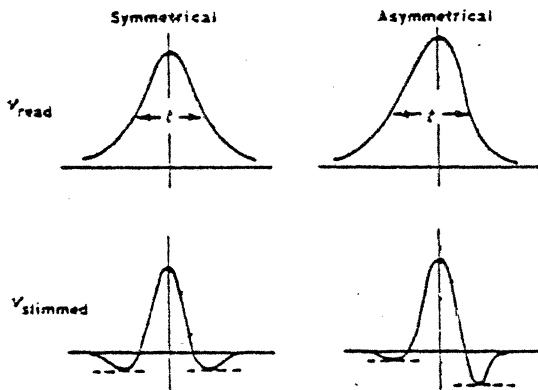


Fig. 18. Comparison of slimmed symmetrical and asymmetrical pulses.